Slobodanka Boljanović

FAILURE PERFORMANCE MODELING OF CYCLICALLY LOADED PLATES WITH EDGE STRESS RAISERS

Abstract. Understanding the surface stress raiser mechanism is of tremendous importance for aerospace and automotive industrial applications at various temporal scales. The present chapter, consequently, discusses the fatigue degradation due to quarter-elliptical corner crack through a novel computational framework. This is sustained by a research on damage tolerance-based residual life coupled with mode intensities and by recommendations on the strategy to define a safety margin design.

Mathematics Subject Classification (2010): Primary: 70-99, 74-99, 70F35, 92C10, 74L10; Secondary: 70Exx, 70KXX, 74M05, 37H20.

Keywords: computational framework, fatigue degradation, quarter-elliptical corner crack, residual life.

Mathematical Institute of the Serbian Academy of Sciences and Arts
Kneza Mihaila 36, 11000 Belgrade, Serbia
slobodanka.boljanovic@mi.sanu.ac.rs

Contents

1. Introduction

Significant increases in load bearing capacities, as well as growing interest in providing functioning at higher-speeds, is placing new and increasing existing fracture mechanics-based demands on large moving systems. In this regard, the need for the development of efficient computational-strategies receives increasing attention, in order to quantify the stress raiser mechanisms in the safety-critical zones with manufacturing/environmental flaws, represented as part-through/quarter-elliptical or semi-elliptical/ crack and through-the-thickness crack.

According to the study by Grandt et al. [1], the fatigue performance of part-through cracks at open and pin-loaded holes has been examined applying the Paris' concept and the finite element method. Atluri and Nishioka [2] have demonstrated that the finite element alternating method can be employed in the stress state analysis of a quarter-elliptical corner crack at pin-loaded hole.

In order to evaluate the stress raiser effects of open hole with the corner crack Vainshok and Varfolomeyev [3] have used the weight function method. Guo [4] has introduced an analytical crack growth model for analyzing the same fatigue damage under biaxial and pin loading. Rigby and Aliabadi [5] have generated the driving mode of quarter-elliptical crack coupled with pin-loaded effect by employing the *J*-integral method and the boundary element method.

Relevant fatigue-critical interaction of the same surface flaws has been investigated by Kim et al. [6] through the Forman crack growth concept [7] with the effective stress-intensity factor and the weight function method. Later, Lanciotti et al. [8] have employed the software frameworks NASGRO and AFGROW together the ABAQUS software framework [9-11] in which the finite element method is implemented.

In the failure assessments for pin loaded configurations, Mikheevskiy et al. [12] have employed the weight function method and the UniGrow software framework based on the Noroozi et al. concept [13]. Boljanović et al. [14] have examined the part-through corner crack at pin loaded hole using the Zhan et al. concept [15] and the *J*-integral method. Then, the durability of the same lug-pin joint with the surface corner crack or through-the-thickness crack has been explored by Boljanović [16] through the stress ratio-dependent crack growth concept [17] coupled with the finite element method [18].

Moreover, the fatigue stability of a quarter-elliptical corner crack or a semi-elliptical crack at the semicircular edge notch has been assessed by Newman et al. [19] and Wu et al. [20] applying the crack closure model together with the finite element method and the weight function method. Through research activities Boljanović et al. [21] have analyzed the failure-critical two notches with either one quarter-elliptical corner crack or through-the-thickness crack combining the Huang-Moan concept [17] and the set of expressions developed by Wu et al. [20] for assessing the stress intensities of crack-like flaws and the finite element method.

From damage tolerance point of view, the fatigue due to surface cracks is still one of the most safety-relevant mechanisms which cannot be avoided in large moving systems. Thus, the failure performance of a quarter-elliptical corner crack is explored in this research study. In order to identify and characterize the potential features of such phenomenon, the analytical framework is proposed, and detailed body of evidence is provided for evaluating of a crack growth progression under fatigue loading. Additionally, by means of novel driving mode expressions, experimentally verified, the effect of crack shape on failure strength of cyclically loaded systems is discussed.

2. Failure Strength Simulation under Cyclic Loading

Complex environment-load history interactions coupled with surface flaws can seriously endanger the efficient functioning of large moving systems. According to fracture mechanics, such stress raisers must be carefully explored through relevant failure concepts [4, 6, 14, 22-27].

Driving mode progression due to the quarter-elliptical corner crack is evaluated in the present research study employing the crack growth law proposed by Zhan et al. [15], which is extended to analyze the part-through corner flaw through two (depth and surface) critical crack directions, as follows:

$$\frac{da}{dN} = C_A \left(e^{\alpha R} \, \Delta K_A \right)^{m_A} \tag{1a}$$

$$\frac{db}{dN} = C_B \left(e^{\alpha R} \, \Delta K_B \right)^{m_B} \tag{1b}$$

where a, b and da/dN, db/dN are crack lengths and corresponding crack growth rates in depth and surface direction, respectively, C_A, m_A, C_B, m_B and ΔK_A, ΔK_B represent relevant material parameters experimentally obtained and stress intensity factors for two critical crack growth directions.

Under cyclic loading the residual strength may be assessed by means of the number of loading cycles *N*, if relevant crack growth rates are integrated from initial a_0, b_0 to final a_f, b_f crack lengths in depth and surface directions, i.e.,

$$N = \int_{a_0}^{a_f} \frac{da}{C_A \left(e^{\alpha R}\, \Delta K_A\right)^{m_A}} \tag{2a}$$

$$N = \int_{b_0}^{b_f} \frac{db}{C_B \left(e^{\alpha R}\, \Delta K_B\right)^{m_B}} \tag{2b}$$

The failure resistance analysis is herein performed through new software program, by employing Euler's algorithm for solving complex-valued life functions (Eq. 2a and Eq. 2b) with respect to two critical crack growth directions.

3. Driving Stress Analysis of Surface Corner Crack

The quantification of the disturbed stress field in safety-critical zones in terms of system durability requires examining the effects of stress raisers associated with service loadings [5, 12, 16, 28-35]. Thus, fatigue response of quarter-elliptical corner crack (Fig. 1, case 1) is herein assessed via the stress intensity factor [36], expressed as follows:

$$\Delta K = F_{qec}\, \Delta S \sqrt{\frac{\pi\, a}{Q}} \tag{3}$$

where ΔK and ΔS are the stress intensity factor range and applied stress range, respectively, Q represents the ellipse shape factor and a is the crack length in depth direction, respectively.

Crack shape variations under cyclic loading are theoretically examined using the correction factor F_{qec}, which can be computed in the case of part-through corner crack [36] using the following fracture mechanics-based expression:

$$F_{qec} = \left(M_1 + M_2 \left(\frac{a}{t}\right)^2 + M_3 \left(\frac{a}{t}\right)^4 \right) g_1\, g_2\, f_\phi\, f_w \tag{4}$$

where t is plate thickness, f_ϕ and f_w are the correction factors involved to generate the angle location effect at the crack front and the effect of plate width, respectively.

Failure mode due to quarter-elliptical crack is herein evaluated combining the effects of crack size, crack shape, front face and thickness of the plate through relevant correction factors, M_1, M_2, M_3, g_1, g_2 ($a/b \geq 1$, Fig. 1) [36], expressed as follows:

$$M_1 = \sqrt{\frac{b}{a}}\left(1.08 - 0.03\frac{b}{a}\right) \tag{5}$$

$$M_2 = 0.375\left(\frac{b}{a}\right)^2 \tag{6}$$

$$M_3 = -0.25\left(\frac{b}{a}\right)^2 \tag{7}$$

$$g_1 = 1 + \left(0.08 + 0.4\left(\frac{b}{t}\right)^2\right)(1 - \sin\phi)^3 \tag{8}$$

$$g_2 = 1 + \left(0.08 + 0.15\left(\frac{b}{t}\right)^2\right)(1 - \cos\phi)^3 \tag{9}$$

Furthermore, the effect of angle location on the crack front and relevant elliptical-crack shape effect are theoretically investigated employing the following expressions:

$$f_\phi = \left(\left(\frac{b}{a}\right)^2 \sin^2\phi + \cos^2\phi\right)^{0.25} \tag{10}$$

$$Q = 1 + 1.464\left(\frac{b}{a}\right)^{1.65}, \ (a/b > 1.0) \tag{11}$$

The influence of plate width associated with thickness and crack shape is taken into account through the finite-width correction factor, given by

$$f_w = 1 - 0.2\lambda + 9.4\lambda^2 - 19.4\lambda^3 + 27.1\lambda^4 \tag{12}$$

$$\lambda = \frac{b}{w}\sqrt{\frac{a}{t}} \ \left(\frac{b}{w} < 0.5\right) \tag{13}$$

where t is the plate thickness and w is width of the plate.

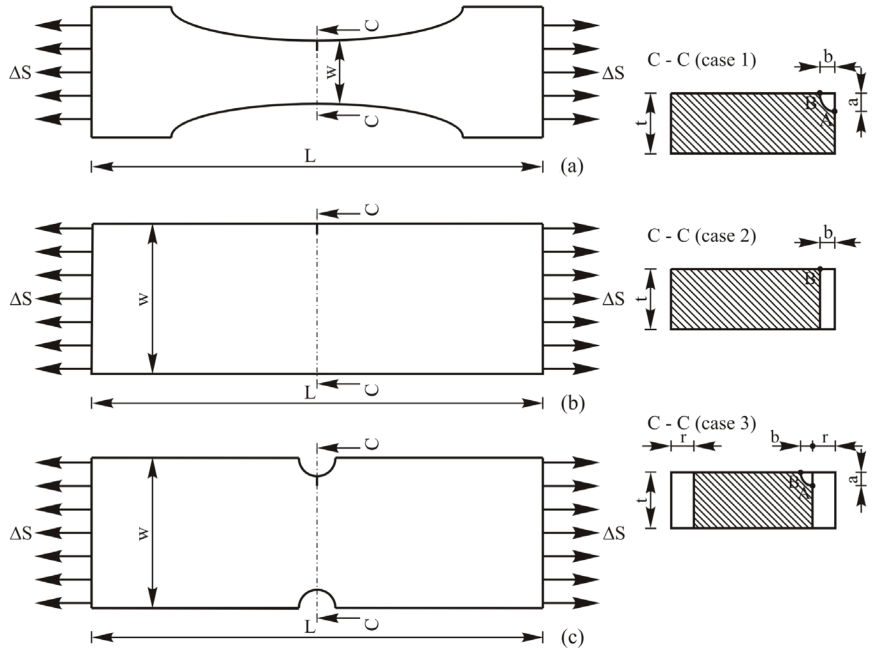

FIGURE 1. Geometry of the plates with quarter-elliptical corner crack (case 1 and case 3) and through-the-thickness crack (case 2).

4. Implementations of Developed Fatigue Design Framework

4.1. Residual Life Estimation of Plates with Crack-Like Corner Flaw. The first section examines the failure resistance of the plate with quarter-elliptical crack (Fig. 1a, case 1) in terms of the number of loading cycles. Such part-through corner crack, located at the edge of the plate made of 2024 T3 (w = 25.4 mm, t = 2.3 mm, C_A= 1.6×10^{-10}, $m_A = m_B$ = 3.39, with da/dN, db/dN in m/cycles and ΔK_A, ΔK_B in MPam$^{0.5}$), is characterized by the following initial lengths in depth and surface crack growth directions: $a_0 = b_0$ = 20 μm. Note that the mode progression is herein analyzed for two values of the stress ratios (R = 0 and -1) coupled with six different maximum stresses, as it is listed in Table 1.

Through damage tolerance-based framework developed, driving forces in the vicinity of crack tip and the number of loading cycles are evaluated in depth and surface crack directions by employing Eq. (3)-(13) coupled with Eq. (2a) and (2b), respectively. Further, relevant life assessments are verified using fatigue experiments discussed by Grover at al. [37], as it is shown in Table 1. Examining those comparisons (in which applied stress ratios are equal to R = 0 and -1) together with corresponding Fig. 2-4 and Fig. 5-7, it can be inferred that fatigue-life assessments adequately correlate with those experimentally obtained for different loading conditions.

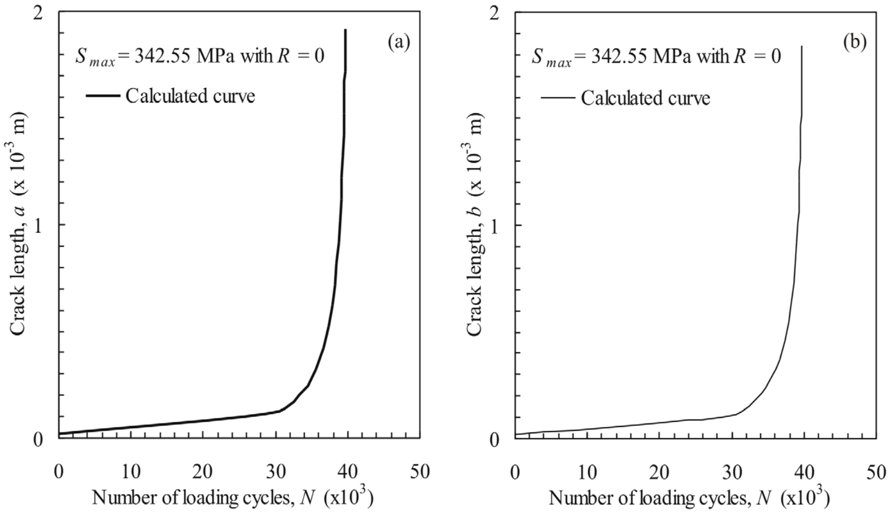

FIGURE 2. Failure analysis of the plate with quarter-elliptical corner crack (S_{max}= 342.55 MPa, R = 0): (a) a versus N and (b) b versus N, calculated curves are the present results.

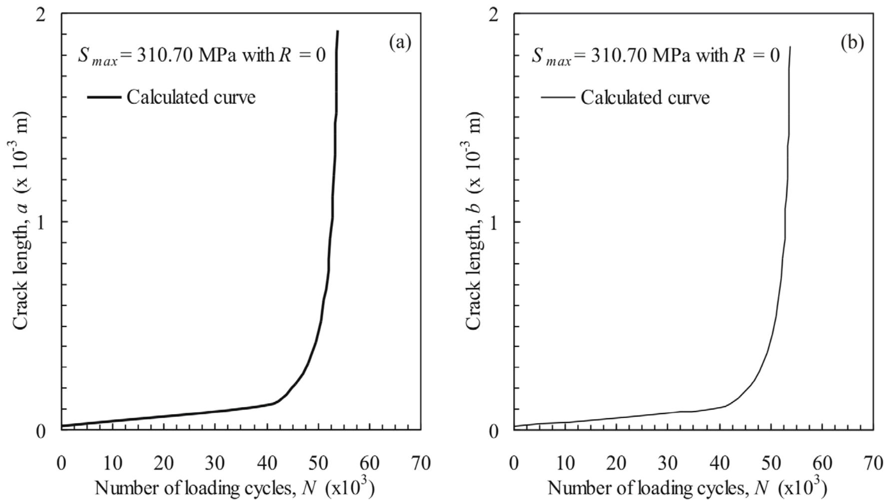

FIGURE 3. Failure analysis of the plate with quarter-elliptical corner crack (S_{max}= 310.70 MPa, R = 0): (a) a versus N and (b) b versus N, calculated curves are the present results.

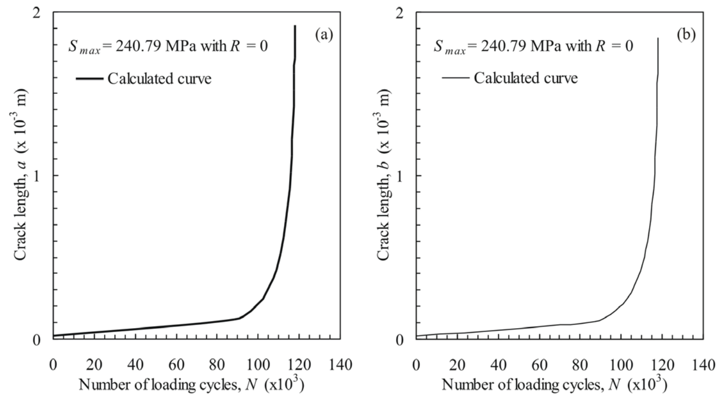

FIGURE 4. Failure analysis of the plate with quarter-elliptical corner crack (S_{max}= 240.79 MPa, R = 0): (a) a versus N and (b) b versus N, calculated curves are the present results.

TABLE 1. Evaluated number of loading cycles and corresponding experimental data, calculations are the present results and experiments are discussed by Grover et al. [37].

R = 0			R = -1		
S_{max} (MPa)	$N^{cal.}$ (cycles)	$N^{exp.}$ (cycles) [37]	S_{max} (MPa)	$N^{cal.}$ (cycles)	$N^{exp.}$ (cycles) [37]
342.55	39700	70000; 79000	273.62	52990	62272; 70000
310.70	53710	81500; 113170	205.21	140500	189423; 276666
240.79	118000	221660	170.64	262600	484210; 575862

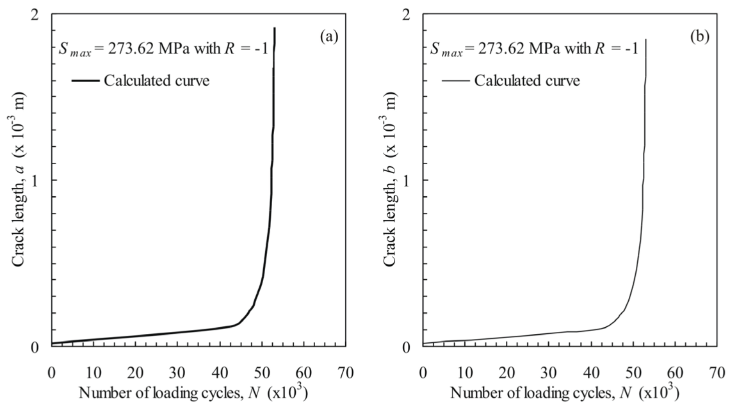

FIGURE 5. Failure analysis of the plate with quarter-elliptical corner crack (S_{max}= 273.62 MPa, R = -1): (a) a versus N and (b) b versus N, calculated curves are the present results.

Moreover, it can be seen in Table 1 that developed computational framework is able to generate the interaction between the effect of stress ratio and the effects of crack-like stress raiser and provides more conservative estimates in the case of stress ratio $R = 0$ (with respect to available experiments [37]). Relevant comparisons shown in Table 1 also indicate that cyclic loadings characterized by negative stress ratio more endanger the failure strength than that with positive-valued stresses.

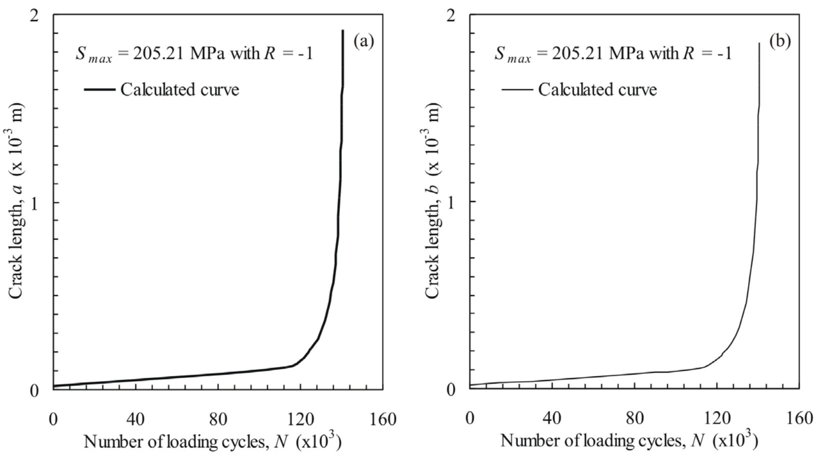

FIGURE 6. Failure analysis of the plate with quarter-elliptical corner crack (S_{max}= 205.21 MPa, R = -1): (a) a versus N and (b) b versus N, calculated curves are the present results.

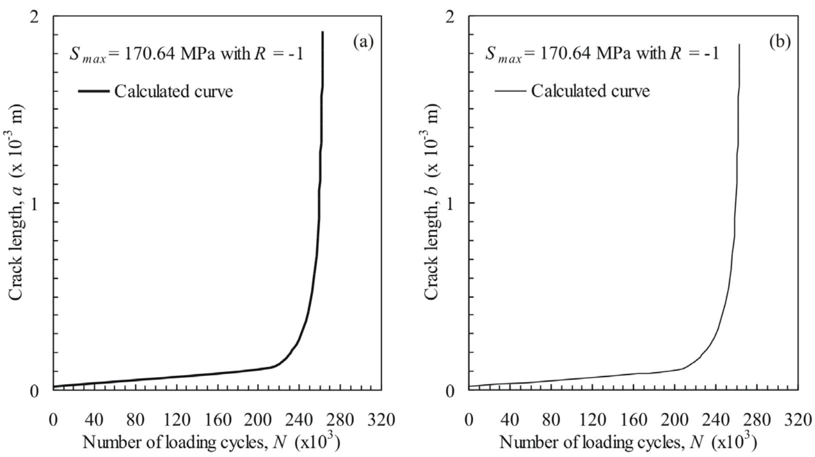

FIGURE 7. Failure analysis of the plate with quarter-elliptical corner crack (S_{max}= 170.64 MPa, R = -1): (a) a versus N and (b) b versus N, calculated curves are the present results.

4.2. Evaluation of Fatigue-Induced Corner Crack. The failure resistance analysis presented here evaluates the crack growth paths under cyclic loading. The stability of the plate (w = 70 mm, t = 9 mm, Fig. 1b, case 1), made of 2024 T3 aluminium alloy, is explored in the case of initial quarter-elliptical corner crack (a_0 = 2.1 mm, b_0 = 1.6 mm). Further, the computational fatigue design is performed by adopting maximum stress equal to S_{max}= 100 MPa with stress ratio R = 0.3 and involving the same material parameters as those employed in section 4.1.

Driving mode progression is theoretically examined by means of the crack growth rate in depth and surface direction employing Eq. (1a) and (1b) together with Eq. (3)-(13). Through such fracture mechanics-based analytical analysis the disturbed stress state was evaluated combining the effect of stress raiser caused by the quarter-elliptical corner crack and the effect of stress ratio. Actually, using computational framework developed for nine different crack lengths in depth direction, relevant crack growth paths were evaluated, as it is shown in Fig.8a and 8b, in which the vertical axis and the horizontal axis coincide with the front face and left side of the plate, respectively.

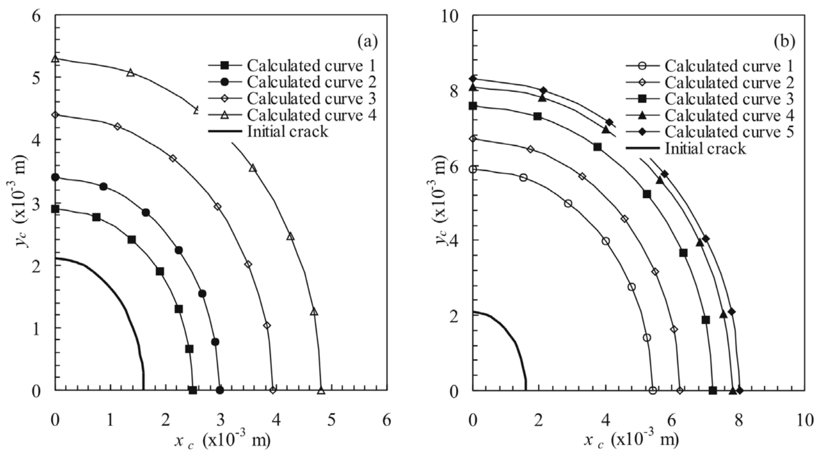

FIGURE 8. Crack growth path evaluations: (a) 1 – a = 2.9 mm, 2 – a = 3.4 mm, 3 – a = 4.4 mm, 4 – a= 5.3 mm and (b) 1 – a = 5.9 mm, 2 – a = 6.7 mm, 3 – a = 7.6 mm, 4 – a = 8.1 mm, 5 – a = 8.3 mm, calculated curves are the present results.

4.3. Failure Performance Estimation of Plates with Edge Stress Raisers. Now, the fatigue strength of plate with a through-crack (Fig.1b, case 2) is tackled through the residual life estimation. The cyclically loaded plate with initial single edge-crack (b_0 = 1.25 mm, w = 60 mm, t = 5 mm, S_{max}= 150 MPa, R = 0) is made of aluminium alloy 2024 T3 (C_B= 1.6×10^{-10}, m_B = 2.96, with da/dN in m/cycles and ΔK in MPam$^{0.5}$).

It is evident that the stress-raiser mechanisms caused by the presence of through-crack and/or part-through crack may seriously jeopardize the durability of large moving systems under service loading. Therefore, the failure of the plate with the through-crack is herein explored by using the following expression for the stress intensity factor:

$$\Delta K = f_{tc}\, \Delta S \sqrt{\pi b} \tag{14}$$

where ΔK and ΔS are stress intensity factor range and applied stress range, respectively, and b denotes the crack length related to through-crack.

Further, the interaction between the effects of disturbed-stress state due to the through-crack and the finite-width effect is theoretically examined by employing the following correction factor:

$$f_{tc} = 1.12 - 0.23\left(\frac{b}{w}\right) + 10.6\left(\frac{b}{w}\right)^2 - 21.7\left(\frac{b}{w}\right)^3 + 30.4\left(\frac{b}{w}\right)^4 \tag{15}$$

where w is the thickness of the damaged plate (Fig. 1b, case 2).

According to fracture mechanics, the fatigue behaviour of a through-crack is analyzed in terms of the crack growth rate and residual life, with respect to the relevant surface crack direction. Thus, through appropriate computational framework in which are implemented Eqs. (14) and (15) together with Eq. (1b) and (2b), the stress raiser effects caused by through-crack are examined. Evaluated stress intensity factor and number of loading cycles, as a function of crack length are shown in Fig. 9a and 9b, respectively.

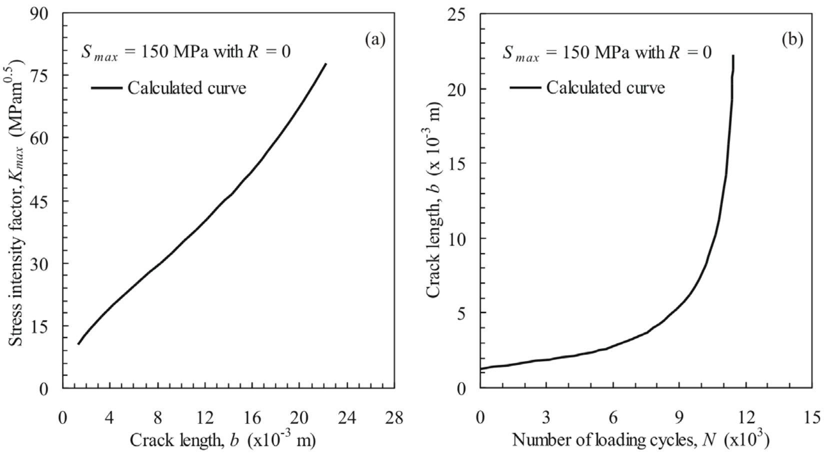

FIGURE 9. Failure analysis of the plate with through-crack: (a) b versus K_{max} and (b) b versus N, calculated curves are the present results.

Moreover, the driving mode analysis presented in this section, estimates the stress-raising power of a quarter-elliptical corner crack at the plate (w = 60 mm, t = 5 mm, Fig. 1b, case 1), whose initial crack lengths are equal to $a_0 = b_0$ = 1.25 mm, respectively, adopting the same cyclic loading (S_{max}= 150 MPa, R = 0) as such in the case of through-crack configuration.

Fatigue-induced damage progression is theoretically herein investigated through the developed computational framework (related to part-through crack) employing Eq. (3)-(13) and Eq. (2a) and (2b), as it was discussed in previous sections. Relevant number of loading cycles generated as a function of crack length in depth and surface direction are shown in Fig. 10a and 10b, respectively.

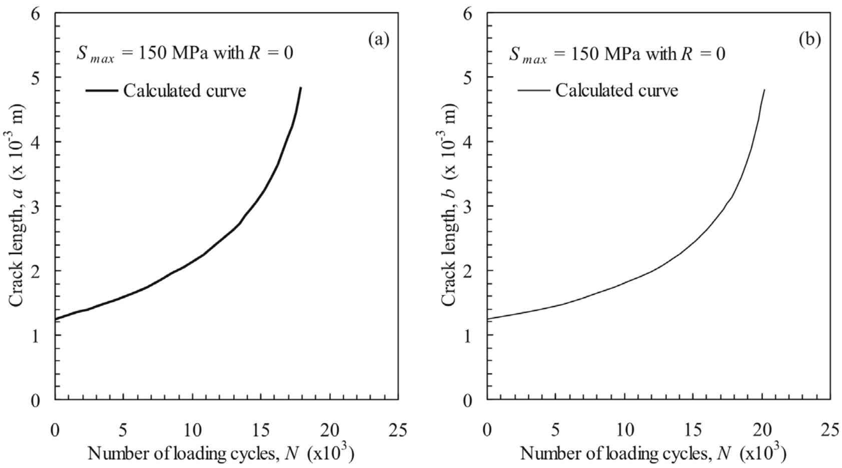

FIGURE 10. Failure analysis of the plate with quarter-elliptical corner crack: (a) a versus N, and (b) b versus N, calculated curves are the present results.

In addition, from appropriate damage tolerance-based evaluations shown in Fig. 9 and Fig. 10 it can be indicated that the detrimental effects due to through-crack threaten the fatigue strength of the plate much more strongly than those caused by part-through crack.

4.4. Stability Analysis of Damaged Plates with/without Notch Effect.

Through this section the stress raising power of quarter-elliptical corner crack is discussed for two damaged plates (Fig. 1b, case 1 and Fig. 1c, case 3). The residual life is estimated in the case of two values of maximum stresses (S_{max}= 68.97 MPa and 91.73 MPa with R = 0.1), and by assuming that the plates (w = 38.1 mm, t = 6.35 mm) are made of aluminium alloy 2024 T3. Under such conditions the plate failure caused by single initial corner crack (whose critical lengths in depth and surface directions are: $a_0 = b_0$ = 1.30 mm and 1.84 mm) is analyzed with and without the inclusion of the effect of two semi-circular edge notches (r = 6.35 mm).

Recently, within research activities realized through the national scientific project OI174001 (2011-2019) supported by the Mathematical Institute of the Serbian Academy of Sciences and Arts and the Ministry of Education, Science and Technological Development of the Republic of Serbia, relevant computational frameworks were developed by the present author and colleagues [14, 16, 21] to analyze and improve time-dependent safety performances of plate-type configurations under complex load/environment in-service interactions, taking into account different stress raiser effects.

Thus, designing against fatigue presented through the previous work [21] examined the plate with two semi-circular edge notches (Fig. 1c, case 3). In such residual strength analysis, the interaction between the notch effect and the effect of quarter-elliptical crack was investigated in terms of the plate life coupled with appropriate stress intensity factors. Relevant failure assessments related to the number of loading cycles, as a function of crack length in depth and surface directions (obtained for the above-mentioned plate with two notches exposed to two levels of maximum stresses), are shown in Fig. 11a and 11b, respectively. Further, in order to estimate the predictive capability of those outcomes, experimentally tested data [38] for the single quarter-elliptical corner crack at the plate with two edge notches are listed in Table 2 and 3 (discussed also in Ref. [21]).

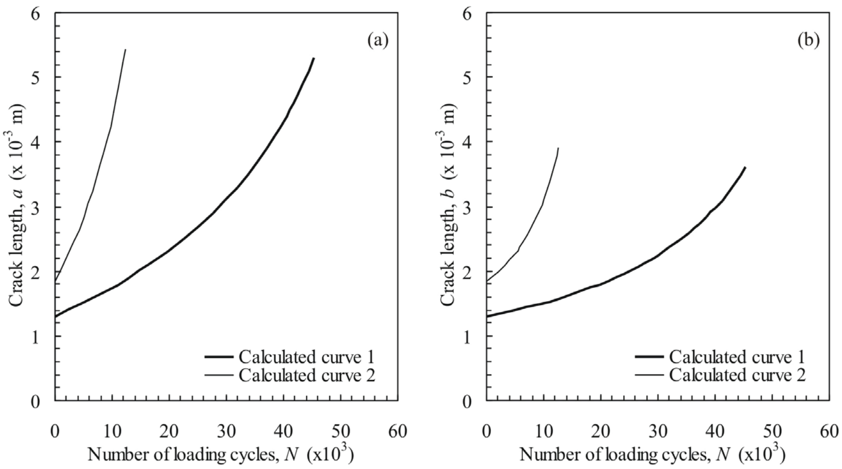

FIGURE 11. Failure analysis of the plate with quarter-elliptical corner crack at the semi-circular notch: (a) a versus N and (b) b versus N (1 – S_{max}= 68.97 MPa and 2 – S_{max}= 91.73 MPa, calculated curves are discussed by Boljanović at al. [21]).

Moreover, the failure of plate with the quarter-elliptical corner crack (Fig. 1a, case 1) was explored under the same loading conditions via the computational framework developed through the present research. Residual life assessments for the damaged plate (a_0 = b_0 = 1.30 mm and 1.84 mm) without notches are shown in Table 2 and 3 for appropriate crack lengths in surface direction and through Fig. 12a and 12b with respect to depth and surface crack direction, respectively.

TABLE 2. Evaluated number of loading cycles and corresponding experimental data, calculations are the present results (S_{max} = 68.97 MPa, $a_0 = b_0$ = 1.30 mm) and experiments are discussed by Everett et al. [38].

S_{max} = 68.97 (MPa)	With two notches		Without notches
b (mm)	$N^{cal.}$ (cycles) [21]	$N^{exp.}$ (cycles) [38]	$N^{cal.}$ (cycles)
2.056	26050	30614	63520
2.540	35510	40070	76450
3.219	42350	47872	86940
3.980	47320	55009	92930

TABLE 3. Evaluated number of loading cycles and corresponding experimental data, calculations are the present results (S_{max} = 91.73 MPa, $a_0 = b_0$ = 1.84 mm) and experiments are discussed by Everett et al. [38].

S_{max} = 91.73 (MPa)	With two notches		Without notches
b (mm)	$N^{cal.}$ (cycles) [21]	$N^{exp.}$ (cycles) [38]	$N^{cal.}$ (cycles)
2.600	7300	9883	14760
3.620	11890	14705	20610
3.830	12420	15100	21630
4.190	13170	17029	22280

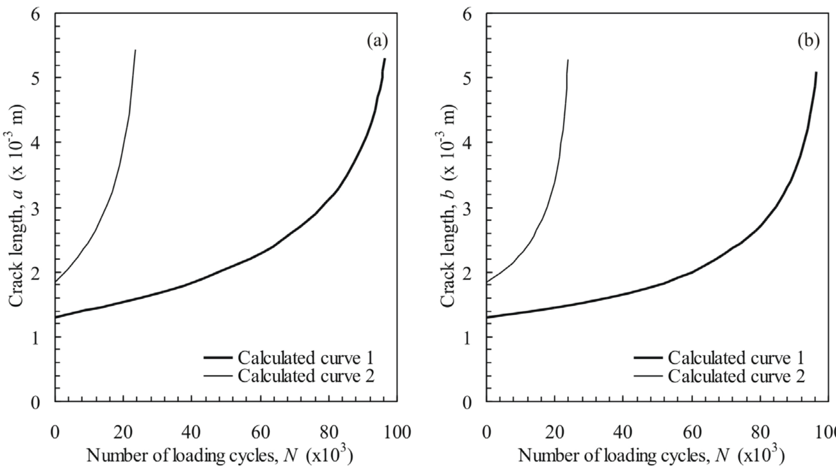

FIGURE 12. Failure analysis of the plate with quarter-elliptical corner crack: (a) a versus N and (b) b versus N (1 – S_{max}= 68.97 MPa and 2 – S_{max}= 91.73 MPa, calculated curves are the present results).

From relevant fatigue analysis presented in this section (by examining Fig. 11 and Fig. 12 together with Table 2 and Table 3), it can be inferred that the stress-raising effects of edge notches associated with the effect of part-through corner crack lead sooner to a serious compromise to the bearing capacity of plate-type configurations than when there is only part-through corner crack. Also, it is evident that the increase applied maximum stress can rather endanger the residual strength under cyclic loading.

4.5. Effects of Crack Shape, Thickness and Width on the Fatigue Degradation of Plates. Finally, the failure resistance is assessed by taking into account the effect of crack shape. Thus, in the case of three different quarter-elliptical corner cracks, characterized by the following depth-to-length ratios a_0/b_0 = 1.196, 1.675 and 2.154, the residual life of the plate (w = 60 mm, t = 5 mm, b_0 = 1.12 mm, Fig. 1b, case 1) was analyzed under cyclic loading (P_{max}= 30000 N, R = 0.1). Note that, the material parameters for 2024 T3 aluminium alloy examined here, are the same as those mentioned in section 4.1.

Stress-raiser phenomenon caused by the quarter-elliptical corner crack at a plate-type configurations is investigated through the stress intensity factor and residual life, using Eq. (3)-(13) and Eq. (2a)-(2b), respectively. In this regard, fatigue assessments generated for three depth-to-length ratios in terms of the number of loading cycles, as a function of crack lengths in depth and surface direction, are shown in Fig. 13a and 13b, respectively.

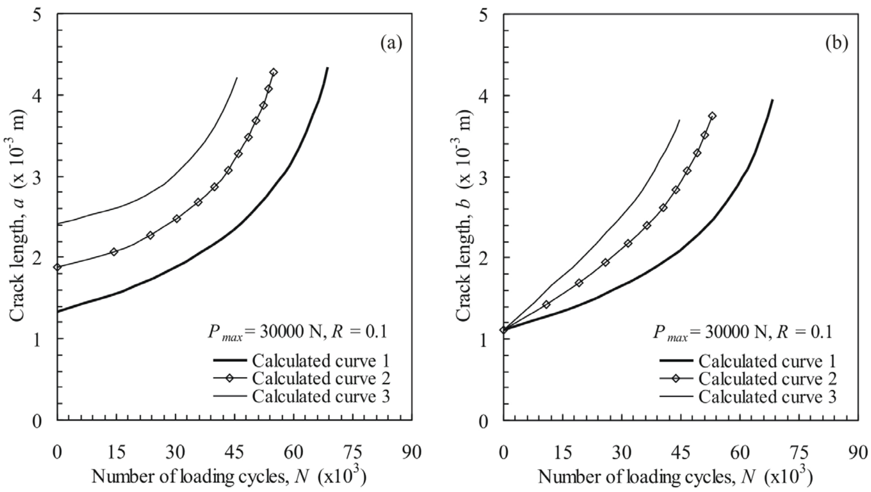

FIGURE 13. Failure analysis of the plate with quarter-elliptical corner crack (b_0 = 1.12 mm): (a) a versus N and (b) b versus N (1 – a_0/b_0 = 1.196, 2 – a_0/b_0 = 1.675, 3 – a_0/b_0 = 2.154, calculated curves are the present results).

Furthermore, the stability of two plates with part-through corner crack (w = 80 mm, a_0 = 1.32 mm, b_0 = 1.16 mm, P_{max}= 20000 N, R = 0.1 and t = 6 mm, a_0 = 1.47 mm, b_0 = 1.23 mm, P_{max}= 45000 N, R = 0.3) was evaluated for three different thicknesses/widths (t = 2.5 mm, 3.25 mm, 4.0 mm and w = 60 mm, 72 mm, 86.4 mm), respectively. Hence, for such thicknesses and plate widths, the number of loading cycles (generated via analytical framework herein developed) is plotted in Fig. 14a, 15a and Fig. 14b, 15b, in the case of two critical crack growth directions.

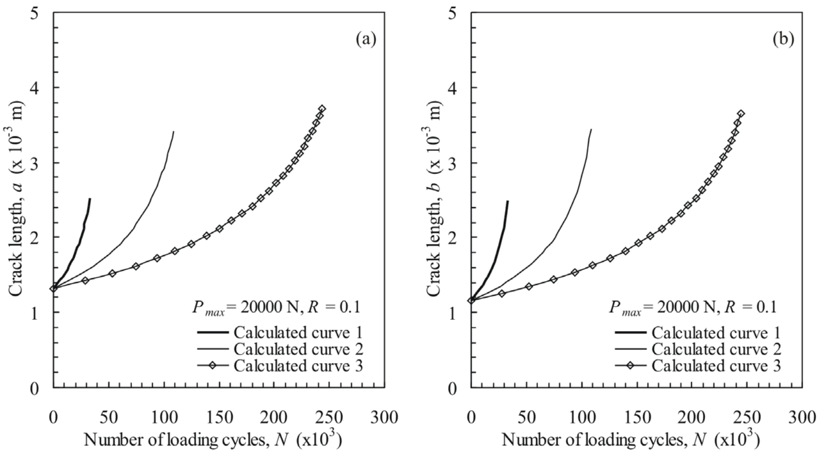

FIGURE 14. Failure analysis of the plate with quarter-elliptical corner crack (w = 80 mm): (a) a versus N and (b) b versus N (1 – t= 2.5 mm, 2 – t= 3.25 mm, 3 – t= 4.0 mm, calculated curves are the present results).

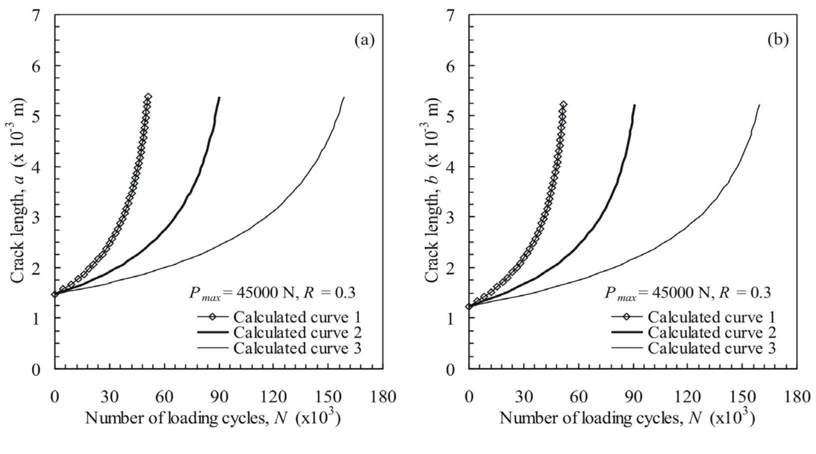

FIGURE 15. Failure analysis of the plate with quarter-elliptical corner crack (t = 6 mm): (a) a versus N and (b) b versus N (1 – w= 60 mm, 2 – w= 72 mm, 3 – w= 86.4 mm, calculated curves are the present results).

Relevant fracture mechanics-based evaluations shown in Fig. 13a and 13b indicate that if the depth-to-length ratio (for part-through corner crack with $a/b \geq 1$) increases, the durability of the large moving systems can be significantly threatened. Also, from Fig. 14a, 14b and Fig. 15a, 15b it can be inferred that the thickness and width must be carefully selected because they play an important role in ensuring safe-integrity performances of damaged plate-type configurations.

5. Conclusions

Demands to assess the durability performance of modern large moving systems are raised to avoid the sudden loss of their resources due to the detrimental effects of manufacturing/environmental flaws under service loadings. Therefore, this research study proposes fracture mechanics-based analytical framework to analyze severity of such crack-like stress raisers by taking into account the effect of stress ratio. Novel expressions generate the changes in the fatigue response, providing a correlation of the stress-intensity variations as well as the residual life with respect to crack lengths in depth and surface directions. Thus, the proposed computational fatigue design tool, experimentally verified, has great potential for a reliable failure strength assessment of plate-type configurations with part-through corner flaws.

Acknowledgement
The research activities presented in this chapter was supported by the Mathematical Institute of the Serbian Academy of Sciences and Arts and the Ministry of Science and Technological Development of the Republic of Serbia within the Project OI174001, which is gratefully acknowledged.

References

[1] Jr.A.F. Grandt, J.A. Harter, D.E. Tritsch, *Semielliptical cracks along holes in plates and lugs* AFWAL-TR-83-3043, Air Force Wright Aeronautical Laboratories, Ohio, United States, 1982.

[2] S.N. Atluri, T. Nishioka, *Computational methods for three-dimensional problems of fracture*, In: S.N. Atluri, (ed.), *Computational Methods in Mechanics of Fracture*, New York, North-Holland Publishing Co., 230-287, 1986.

[3] V.A. Vainshok, I.V. Varfolomeyev, *Stress intensity factor analysis for part-elliptical cracks in structures*, International Journal of Fracture **46** (1990), 1-24.

[4] W. Guo, *Stress intensity factors for corner cracks at holes subjected to biaxial and pin loads*, Engineering Fracture Mechanics **46** (1993), 473-479.

[5] R. Rigby, M.H. Aliabadi, *Stress intensity factors for cracks at attachment lugs*, Engineering Failure Analysis **4**(2) (1997), 133-146.

[6] J.H. Kim, S.B. Lee, S.G. Hong, *Fatigue crack growth behavior of Al7050-T7451 attachment lugs under flight spectrum variation*, Theoretical and Applied Fracture Mechanics **40**(2) (2003), 135-144.

[7] R.G. Forman, V.E. Kearney, R.M. Engle, *Numerical analysis of crack propagation in cyclic-loaded structures*, Transactions of the ASME, Journal of Basic Engineering **89** (1967), 453-464.

[8] A. Lanciotti, F. Nigro, C. Polese, *Fatigue crack propagation in the wing to fuselage connection of the new trainer aircraft M346*, Fatigue & Fracture of Engineering Materials & Structures **29**(12) (2006), 1000–1009.

[9] *NASGRO 4.02 Fracture mechanics and fatigue crack growth analysis software,* NASA Johnson Space Center and Southwest Research Institute, United States, 2002.

[10] *AFGROW Reference Manual. Wright-Patterson Air Force Base*, AFRL/VASM, United States, 2003.

[11] *ABAQUS Version 6.4. Copyrights c Hibbitt*, Karlsson & Sorensen, Italy, 2003.

[12] S. Mikheevskiy, G. Glinka, D. Algera, *Analysis of fatigue crack growth in an attachment lug based on the weight function technique and the UniGrow fatigue crack growth model*, International Journal of Fatigue **42** (2012), 88-94.

[13] A.H. Noroozi, G. Glinka, S. Lambert, *A study of stress ratio effects on fatigue crack growth using the unified two-parameter fatigue crack growth driving force*, International Journal of Fatigue **29** (2007), 1616-1633.

[14] S. Boljanović, S. Maksimović, A. Carpinteri, B. Jovanović, *Computational fatigue analysis of the pin-loaded lug with quarter-elliptical corner crack*, International Journal of Applied Mechanics **9** (2017), 1750058.

[15] W. Zhan, N. Lu, C. Zhang, *A new approximate model for the R-ratio effect on fatigue crack growth rate*, Engineering Fracture Mechanics **119** (2014), 85-96.

[16] S. Boljanović, *Computational modeling of aircraft lugs failure under fatigue loading*, International Journal of Fatigue **114** (2018), 252–261.

[17] X. Huang, T. Moan, *Improved modeling of the effect of R-ratio on crack growth rate*, International Journal of Fatigue **29** (2007), 591-602.

[18] *MSC/NASTRAN software code. Theoretical manuals*. The MacNeal-Schwendler Corporation, Los Angeles, United States, 1994.

[19] Jr.J.C. Newman, E.P. Phillips, M.H. Swain, *Fatigue-life prediction methodology using small-crack theory*, NASA Technical Memorandum 110307, National Aeronautics and Space Administration, Langley Research Center, Hampton, Virginia, United States, 1997.

[20] X.R. Wu, J.C. Newman, W. Zhao, M.H. Swain, C.F. Ding, E.P. Phillips, *Small crack growth and fatigue life predictions for high-strength aluminium alloys part 1 - experimental and fracture mechanics analysis*, Fatigue & Fracture of Engineering Materials & Structures **21** (1998), 1289–1306.

[21] S. Boljanović, S. Maksimović, A. Carpinteri, M. Ćosić, *Fatigue endurance design of plates with two semicircular edge notches and one quarter-elliptical corner crack or through-the-thickness crack*, International Journal of Fatigue **127** (2019), 45–52.

[22] A. Carpinteri, *Handbook of Fatigue Crack: Propagation in Metallic Structures*, Elsevier Science B.V., Amsterdam, the Netherlands, 1994.

[23] R. Jones, D. Peng, S. Pitt, C. Wallbrink, *Weight functions, CTOD and related solutions for cracks at notches*, Engineering Failure Analysis **11** (2004), 79-114.

[24] P.S. Song, Y.L. Shieh, *Crack growth and closure behaviour of surface cracks*, International Journal of Fatigue **26** (2004), 429-436.

[25] S. Boljanović, S. Maksimović, *Fatigue crack growth modeling of attachment lugs*, International Journal of Fatigue **58** (2014), 66–74.

[26] S. Boljanović, S. Maksimović, M. Djurić, *Fatigue strength assessment of initial semi-elliptical cracks located at a hole*, International Journal of Fatigue **92** (2016), 548–556.

[27] S. Boljanović, S. Maksimović, *Fatigue failure analysis of pin-loaded lugs*, Frattura ed Integrità Strutturale **35** (2016), 313-321.

[28] Y. Yamashita, M. Shinozaki, Y. Ueda, K. Sakano, *Fatigue crack growth life prediction for surface crack located in stress concentration part based on the three-dimensional finite element method*, ASME Journal of Engineering for Gas Turbines and Power **126** (2004), 160-166.

[29] A. Carpinteri, R. Brighenti, S. Vantadori, *Notched shells with surface cracks under complex loading*, International Journal of Mechanical Sciences **48** (2006), 638-649.

[30] A. Carpinteri, R. Brighenti, S. Vantadori, *Notched double-curvature shells with cracks under pulsating internal pressure*, International Journal of Pressure Vessels and Piping **86** (2009), 443-453.

[31] A. Carpinteri, R. Brighenti, S. Vantadori, *Influence of the cold-drawing process on fatigue crack growth of a V-notched round bar*, International Journal of Fatigue **32** (2010), 1136-1145.

[32] N. Antoni, F. Gaisne, *Analytical modellng of static stress analysis of pin-loaded lugs with bush fitting*, Applied Mathematical Modelling **35** (2011), 1-21.

[33] I. Vasović, S. Maksimović, K. Maksimović, S. Stupar, G. Bakić, M. Maksimović, *Determination of stress intensity factors in low pressure turbine rotor disks*, Mathematical Problems in Engineering **2014** (2014), 304638.

[34] S. Boljanović, A. Carpinteri, *Modelling the residual strength of fatigue damage at a single semicircular edge notch: Semielliptical crack and through-the-thickness crack*, Fatigue & Fracture of Engineering Materials & Structures **42** (2019), 1010–1021.

[35] S. Boljanović, *Fatigue performance evaluation for crack-like surface flaws*, International Journal of Fatigue **124** (2019), 371–379.

[36] Jr.J.C. Newman, I.S. Raju, *Stress-intensity factor equations for cracks in three-dimensional finite bodies subjected to tension and bending loads*, NASA Technical Memorandum **85793**, National Aeronautics and Space Administration, Langley Research Center, Hampton, Virginia, United States, 1984.

[37] H.J. Grover, W.S. Hyler, P. Kuhn, C.B. Landers, F.M. Howell, *Axial-load fatigue properties of 24S-T and 75S-T aluminium alloy as determined in several laboratories*, NASA Technical Memorandum **2928**, National Aeronautics and Space Administration, Langley Research Center, Hampton, Virginia, United States, 1953.

[38] R.A. Everett Jr.W.T. Matthews, R. Prabhakaran, Jr.J.C. Newman, M.J. Dubberly, *The effects of shot and laser peening on fatigue life and crack growth in 2024 aluninum alloy and 4340 steel*, NASA Technical Memorandum 2001-210843, National Aeronautics and Space Administration, Langley Research Center, Hampton, Virginia, United States, 2001.